



REEVALUATING NOISE SOURCES APPEARING ON THE AXIS FOR BEAMFORM MAPS OF ROTATING SOURCES

Csaba HORVÁTH¹, Bence TÓTH¹, Péter TÓTH²,
Tamás BENEDEK¹, János VAD¹

¹ *Budapest University of Technology and Economics,
Faculty of Mechanical Engineering, Department of Fluid Mechanics,
1111 Budapest, Bertalan Lajos utca 4-6, Hungary*

² *CFD.HU Ltd., 1027 Budapest, Medve utca 24, Hungary*

SUMMARY

This paper presents a beamforming investigation that focuses on the noise source appearing on the axis of turbomachinery. Until now these noise sources were often disregarded during beamforming investigations, as they were associated with motor noise. With the help of the Mach radius concept, it is shown that the noise source is not only resulting from motor noise, but also from other noise sources which are located at other radial positions. This shows the importance of understanding these noise sources in order to accurately evaluate beamforming results of rotating noise sources. The results of the investigation also provide the basis of a new beamforming method designed specifically for rotating coherent noise sources.

INTRODUCTION

As legislations and regulations have become more stringent along with the expectations of customers, the amount of research in the field of turbomachinery aeroacoustics has progressively increased. As a result of this, turbomachinery design requirements are continuously evolving, often pushing the limits of design practices. The drive to further increase efficiency and reduce noise levels is also pushing technology to develop at a fast pace. Design, simulation, and measurement technologies are therefore being refined and even radically reformed in the process. With regard to acoustic measurement technology, microphone technology has been improved, measurement techniques have been developed, and a combination of the two has helped us gain more information from the recorded acoustic data than ever before possible.

Traditionally, microphones have been set up and recorded individually, with the spectrum of the individual microphone signals providing a vast amount of information regarding the radiated noise field of the investigated phenomena. The development of phased array microphone beamforming technology has made it possible to extend these capabilities, simultaneously recording multiple microphone signals and then processing the results in order to learn more about the noise sources which are being investigated. Beamforming processes developed specifically for rotating sources have provided a nonintrusive means by which the noise sources of turbomachinery can be localized. Utilizing phased array microphones and these advanced beamforming algorithms we are able to collect data for identifying turbomachinery noise sources, which is becoming a common practice [1-4]. On the other hand, the results are not so easily understood. Most beamforming algorithms assume that the noise is generated by compact incoherent noise sources, in most cases resulting in beamform maps which localize the noise sources to their true locations. If the investigated noise sources are coherent, the beamforming algorithms often have a hard time distinguishing one source from the other, resulting in the noise sources incorrectly being located on the map. With regard to rotating coherent noise sources, the publications of Horváth et al. have shown that the noise sources are pinpointed to their respective Mach radii rather than their true noise source locations [5].

In this investigation, beamform maps for a synthetic axial flow fan test case are investigated from the axial direction. The focus of the investigation is the noise source appearing on the axis of the fan. In many similar investigations, noise sources located on the axis have been associated with motor noise [1, 4]. Taking into account what is now known about rotating coherent noise sources appearing at their respective Mach radii, it is shown here that the noise sources appearing on the hub can, in some cases, be resulting from noise sources located on the rotors or even on the guide vanes, depending on how the results are processed. An explanation is provided as to why these noise sources appear on the axis, and information is given as to their true noise source locations. This investigation is motivated by a desire to better understand this phenomenon, which is necessary in order to accurately process beamforming results of rotating coherent as well as incoherent noise sources, and which provides the basis of a new beamforming investigation method designed specifically for the investigation of rotating coherent noise sources.

TURBOMACHINERY NOISE SOURCES

In categorizing turbomachinery noise sources, they can be split into two main groups, tonal and broadband noise sources. Tonal noise sources are characterized by a discrete frequency, and are associated with the regular cyclic motion of the rotor blades with respect to a stationary observer and with the interaction of the rotors with adjacent structures [6]. These are referred to as Blade Passing Frequency (BPF) tones and interaction tones, respectively. Broadband noise sources are characterized by a wide frequency range, and are associated with the turbulent flow in the inlet stream, boundary layer, and wake [6]. With respect to the present investigation, the coherence of the noise sources also needs to be taken into consideration. Coherent noise sources are characterized by a time invariant phase relationship. While by definition broadband noise cannot be coherent, many tonal turbomachinery noise sources often are.

AXIAL FLOW FAN TEST CASE

In this investigation a synthetic axial flow fan test case is presented. The synthetic fan is used instead of a real fan in order to provide a means by which multiple noise sources can individually be investigated. The left side of Figure 1 provides a schematic of the fan test case which is synthesized herein. An axial flow fan having 15 rotor blades (only 5 are pictured in order to make the figure clear) and 1 downstream guide vane is investigated by a microphone phased array located 0.3 m in the upstream axial direction. The diameter of the phased array is 1m. The fan has a diameter of 0.4

m and is rotated at -12000 RPM (-200 rev/s). In this way the investigated frequency is maximized while keeping the blade tip velocity subsonic. It is evident that this is not a common fan test case, but is used in order to provide representative data which can easily be created and processed with the available technology.

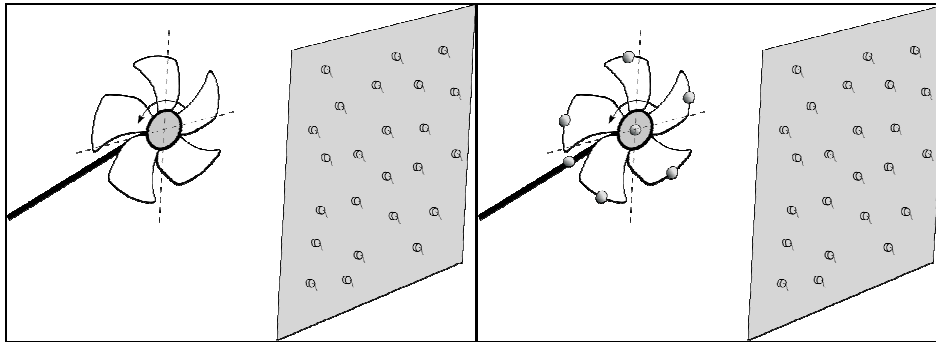


Figure 1: Schematic of the fan test case which is synthesized in the investigation (left) and the synthetic fan test case, with monopole noise sources replacing the rotors, guide vane and motor (right)

The following three components of turbomachinery noise are investigated: motor noise, guide vane noise radiating from the guide vanes as they interact with the rotors, and rotor noise radiating from the rotors as they interact with the guide vanes. The motor is represented by 1 stationary monopole noise source located on the axis. The guide vane is represented by 1 stationary monopole noise source located at the blade tip, and the rotors are represented by 15 coherent rotating monopole noise sources located at the blade tips. The right side of Figure 1 shows a schematic of the monopole noise sources which replace the true noise sources. They are represented by small spheres in the figure, and out of the 15, only 5 rotor noise sources are shown, in order to improve the clarity of the figure.

In order to account for the limited resolution of the finite aperture array, the investigated frequency is chosen as 3000 Hz. The parameters of the synthetic axial flow fan test case are set accordingly, and therefore the results provide beamform maps which clearly depict the investigated noise sources. The stationary monopole noise source located on the axis and representing the motor radiates at 3000 Hz, and should be considered as a harmonic of the motor noise. The stationary monopole noise source representing the guide vane also radiates at 3000 Hz, as the potential field and/or the viscous wake of the 15 rotor blades rotating at -12000 RPM interact with the guide vane. The 15 coherent rotating monopole noise sources located at the blade tips and representing the rotors radiate at 3000 Hz, which is the 15th harmonic of the potential field and/or viscous wake of the guide vane interacting with the rotor blades. The magnitude of each noise source was taken as equal for demonstration purposes.

MEASUREMENT SETUP

The synthetic measurement test case (referred to as measurement) is produced by two monopole noise sources. One is located on the axis and radiates at a frequency of 3000 Hz. This noise source represents the motor and is stationary in both the absolute as well as the rotating reference frame. The other is located at a radius of 0.2 m and radiates at a frequency of 3000 Hz. It represents the guide vane and is stationary in the absolute reference frame, while rotating around the axis at 12000 RPM in the rotating reference frame. The measurement setup can be seen in Figure 2.

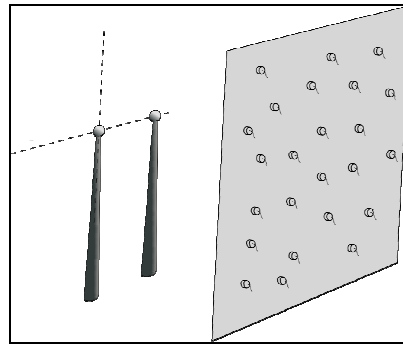


Figure 2: Synthetic measurement test case

SIMULATION SETUP

The synthetic simulation test case (referred to as simulation) is produced by three types of noise sources. The first is located on the axis and radiates at a frequency of 3000 Hz. As in the case of the measurement, this noise source represents the motor and is stationary in both the absolute as well as the rotating reference frame. The second noise source is located at a radius of 0.2 m and radiates at a frequency of 3000 Hz. It represents the single downstream guide vane and is stationary in the absolute reference frame, while rotating around the axis at 12000 RPM in the rotating reference frame. The third consists of 15 coherent noise sources which are evenly distributed around the axis at a radius of 0.2 m. These noise sources represent the 15 rotor blades and are radiating at a frequency of 3000 Hz while rotating at -12000 RPM in the absolute reference frame. In the rotating reference frame these noise sources are stationary. A schematic of the simulation test case can be seen on the right side of Figure 1. Note that the figure does not show all 15 rotor noise sources, in order to make the figure easier to understand.

BEAMFORMING

The acoustical measurements are performed using the Optinav Inc. Array 24: Microphone Phased Array System. The microphones of the system are arranged along a logarithmic spiral and mounted on an aluminum plate. This system provides the hardware for carrying out the measurements, with the phase difference measured between the microphone signals providing the information which is needed for localizing the noise sources with beamforming algorithms [7]. For the simulation, in-house virtual noise source generation and propagation software is used for creating the virtual microphone signals at the same 24 microphone positions. The in-house code is able to produce noise sources which are moving at subsonic speeds, while taking into account the Doppler Effect. Both the measurement and the simulation data is processed by versatile in-house beamforming software. Two types of algorithms are used: the classical frequency-domain based Delay & Sum (DS) method [7], which can localize stationary sources in an absolute reference frame, and the Rotating Source Identifier (ROSI) method [1], which can localize the sources which are stationary in a rotating reference frame. The results provide beamform maps, which display the magnitudes and the positions of the strongest sources located in the investigated plane for a given frequency range. Using these two algorithms, the sound sources originating from both the stationary and rotating elements of the fan can be localized.

Beamforming, in essence, utilizes the phase differences measured between the microphone signals to determine the direction of arrival of the wave fronts. By adjusting the phase shifts (time delays) of the microphone signals relative to each other, a maximum correlation can be obtained between them. The corresponding phase shifts give information as to the direction of arrival of the wave fronts and hence the locations of the noise sources. This forms the basis of the DS beamforming method [7]. The method can be considered as forming a sensitivity curve, called mainlobe that is

directed toward possible compact monopole noise source positions by phase adjustments. These possible source positions are defined by the user, providing focus points for the beamforming methodology, and the beamform maps display the strengths of the investigated sources.

The ROSI beamforming method is an extension of the DS method for rotating source models [1]. The main difference between the two methods is that the ROSI method applies a so called deDopplerization step in order to place the rotating noise sources into a rotating reference frame and hence make them stationary. The positions and velocities of the possible noise sources are accounted for by correcting the time difference and amplitude data with regard to each receiver position. The corrected source signals are then processed with a beamforming method that corresponds with the DS method. For a more detailed description of the ROSI method, see reference [1]. A more detailed description of the phased array microphone system and of the beamforming algorithms applied in the in-house code is available in [4].

In general, beamforming methods developed for rotating noise sources, such as the ROSI method [1] and the Rotating Beamforming method [2] are very useful for investigating rotating incoherent noise sources. In examining the test cases that are provided in [1-2], it can be seen that the investigators took this into account and investigated rotating broadband noise sources and rotating incoherent tonal noise sources. On the other hand, if one wants to look at cases where both coherent and incoherent noise sources are present, the effect of the coherent noise sources need to be accounted for.

MACH RADIUS

Coherent noise sources often give misleading beamforming results. The interaction patterns of the wave fronts make it hard to distinguish one noise source from another by most beamforming methods. The interaction patterns of rotating coherent noise sources also give misleading results, as the apparent sources do not show where the actual noise sources are located, but rather point to the Mach radius [5]. The name “Mach radius” or “sonic radius” refers to the mode phase speed, the speed at which the lobes of the given mode rotate around the axis, having a Mach number of 1 at the Mach radius (z^* , a normalized radius, where $z^* = 1$ refers to the blade tip) when examined from the viewpoint of the observer [8]. For turbomachinery applications, the Mach radius is calculated using Equation 1, with n being the harmonic index, B being the blade count or guide vane count, M_t being the blade tip Mach number, M_x being the flow Mach number, and Θ being the angle of the viewer with regard to the axis (upstream direction referring to 0°), with subscripts 1 and 2 referring to the rotor or guide vane of the acoustic harmonic and loading harmonic, respectively. The equation is formulated for a turbomachinery system consisting of two rotors or one rotor and one guide vane which are moving relative to one another. Acoustic harmonic refers to the rotor or guide vane which is radiating noise while being loaded by the potential field and/or the viscous wake of the other, which is referred to as the loading harmonic. Both rows of rotors or guide vanes need to be considered as acoustic as well as loading harmonics in order to receive a complete and accurate sound field, since each blade row loads the other blade row and also radiates sound simultaneously [8].

$$z^* = \frac{(n_1 B_1 - n_2 B_2)}{(n_1 B_1 M_{t1} + n_2 B_2 M_{t2})} \frac{(1 - M_x \cos \Theta)}{\sin \Theta} \quad (1)$$

Examining the Mach radius equation for the case presented in this study leads to some interesting conclusions. The first thing that can be noticed is that examining the system from the axial direction leads to $\sin \Theta = 0$. This would be true in an idealized case, if only a single microphone were used, but since 24 microphones are used, none of which are located exactly on the axis, $\Theta \neq 0^\circ$. A value

of $\Theta = 1^\circ$ was used for the calculation of the Mach radius with regard to an angle representative of the center of the array, as was done in [5].

The next point of interest is with regard to those interaction tones that result in a Mach radius that is equal to zero, or in other words, when the noise source aligns with the axis of rotation. For cases of subsonic flow, this can occur when $(n_1 B_1 - n_2 B_2) = 0$, as can be seen in Equation 1. In the test case presented here, this will happen when the 1st harmonic of the 15 blade rotor and the 15th harmonic of the single guide vane are investigated at their interaction frequency of 3000 Hz. The azimuthal mode number (m) provides some physical meaning as to what a Mach radius of zero means (see Equation 2) [9-10]. The azimuthal mode number gives the number of pressure lobes that are rotating azimuthally around the axis as a result of the rotating potential field and viscous wake of the blades and their interactions with adjacent structures [9-10]. For the case of $m = 0$ there are no azimuthal lobes rotating around the axis, and similarly to duct acoustics, this results in axial modes that produce plane waves which propagate in the axial direction [11].

$$m = |n_1 B_1 - n_2 B_2| \quad (2)$$

PLANE WAVES

Though the mode pertaining to $m = 0$ produces plane waves, it is known from the literature that plane waves that behave as prescribed by their model equations can only be produced in cylindrical ducts at low frequencies [12]. The literature also states that plane waves can be considered as behaving as spherical waves that are examined at a large distance from their source, or as spherical waves which are examined in a space of small extent as compared to the distance from the source [12]. In the fan test case, the plane waves are produced by a finite number of coherent sources which are evenly distributed around the circumference of the unducted synthetic axial flow fan test case. The wave front should therefore only be considered as a plane wave if investigating the circumferentially distributed coherent noise sources from a small distance with a phased array that has a smaller diameter than the noise source, or if investigating the wave front from a large distance. In our case, the array is located relatively close to the source, but the diameter of the array is relatively large as compared to the noise source. The wave fronts are therefore not expected to behave as planar waves.

In order to visualize what would happen if truly planar waves, the wave fronts of which are parallel to the plane of the array, were investigated with the applied beamforming methods, a simulated synthetic plane wave test case is examined here with the DS method. In general, the DS method assumes that compact monopole noise sources are being investigated, and therefore should not be able to localize noise sources in planes that are very close to it. The plane waves are produced by the same in-house code used to create the simulation case of the axial fan test case. The results can be seen in Figure 3. The DS method is used to try and localize noise sources in multiple planes located at various distances from the phased array as a function of array diameter. These are 0.5 array diameters (left side of Figure 3), 1 array diameter (middle of Figure 3), and 10 array diameters (right side of Figure 3). Assuming that the source is located at a close distance (such as 0.5 array diameters), the beamform maps show only sidelobes, artificial noise sources resulting from the beamforming process, while assuming that the noise sources are located farther away, the beamform maps localize the noise source to the middle of the investigated plane. As discussed above, beamforming is akin to determining the normal to the wave front at the microphone positions and tracing those back to their origin. Therefore, for a plane wave that is investigated by a beamforming method that is looking for monopole noise sources located far away from the phased array, the beamform map should locate the noise source to the center of the investigated plane.

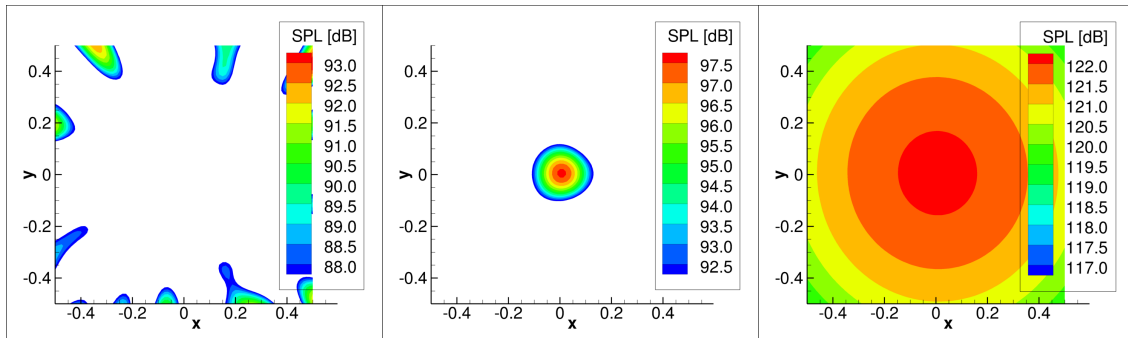


Figure 3: Investigation of plane waves using the Delay & Sum beamforming algorithm, assuming that the source is located at different distances: $0.5 D$ (left), D (middle), $10 D$ (right)

RESULTS

As stated in the introduction, the focus of this investigation is the noise source appearing on the axis of the fan. These noise sources are often neglected during the investigations, as they are associated with motor noise, as seen in [4] and [1]. Mach radius calculations show that these noise sources are not necessarily related to motor noise, suggesting that they should be further investigated. The measurement and simulation test cases investigated here are designed to prove this point by providing an opportunity for investigating each noise source separately. Each noise source is investigated in an absolute as well as rotating reference frame with the help of the DS and ROSI methods.

The first noise source to be presented is that of motor noise in the absolute reference frame. Figure 4 presents both the measurement (left side) and simulation (right side) beamform maps of the narrow band frequency range pertaining to 3000 Hz. The measurement results are realized by the DS method and the simulation results are realized by the ROSI method, since the simulation was created in the rotating reference frame while the measurement was executed in the absolute reference frame. The application of the DS or ROSI methods, as a result of differing reference frames, does not cause any significant discrepancies in the results, as can be seen here. As would be expected from the results, the noise sources are localized to their true noise source locations. It should be noted that the measurement and simulation tests are independent of one another and the levels are therefore not expected to agree.

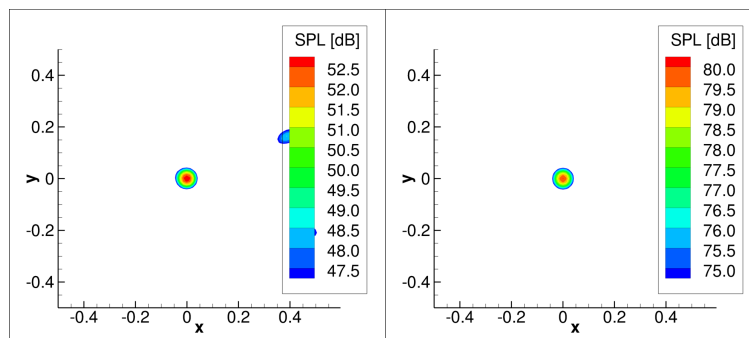


Figure 4: Absolute reference frame beamform maps of the motor noise source: Measurement case (left) and Simulation case (right)

In the absolute reference frame a single guide vane also radiates sound at a frequency of 3000 Hz as it is loaded by 15 rotor blades rotating at 12000 RPM (200 rev/s). Figure 5 presents both the measurement (left side) and simulation (right side) beamform maps for this case. The measurement results are realized by the DS method and the simulation results are realized by the ROSI method. The results show that the stationary noise sources are once again localized to their true noise source locations. As seen in Figures 1 and 2, the guide vanes in the two cases are located in different

locations. The guide vane in the measurement is located at coordinate $[0, 0.2]$, while in the simulation it is located at approximately $[-0.16, -0.12]$. The position of the guide vane in the simulation results depends on what position the ROSI method rotated all the results to during the beamforming process. Starting the processing of the results at an earlier or later time step would rotate the noise source to a different position along the circumference.

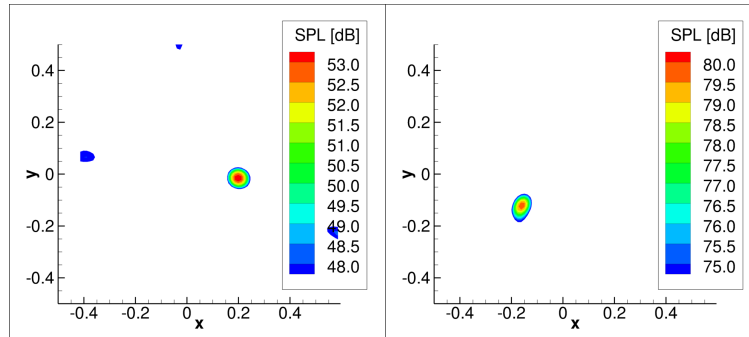


Figure 5: Absolute reference frame beamform maps of the guide vane noise source: Measurement case (left) and Simulation case (right)

When the 15 rotor blades pass the guide vane, they are loaded by the guide vane at a frequency of 200 Hz. The 15th harmonic of this loading also radiates at 3000 Hz. The reason for investigating the 15th harmonic is that it is the harmonic which will produce an interaction tone that is located on the axis according to the Mach radius calculations. The left side of Figure 6 presents the beamform map of these rotating noise sources when investigated in the absolute reference frame by the ROSI method. Only simulation results are shown, since no measurement data is available for this case. Contrary to what would be expected if the Mach radius calculations are not taken into consideration, there is only a single noise source located on the axis of rotation. Taking into consideration what we know about Mach radius, the noise source is correctly located on the axis since the 15 coherent noise sources produce sound waves that add up constructively or destructively producing a wave front similar to a plane wave within the extent of the noise source. When investigated with a relatively large array that is located at a relatively large distance, the wave front will be comprehended by the beamforming process as coming from a monopole noise source located on the axis.

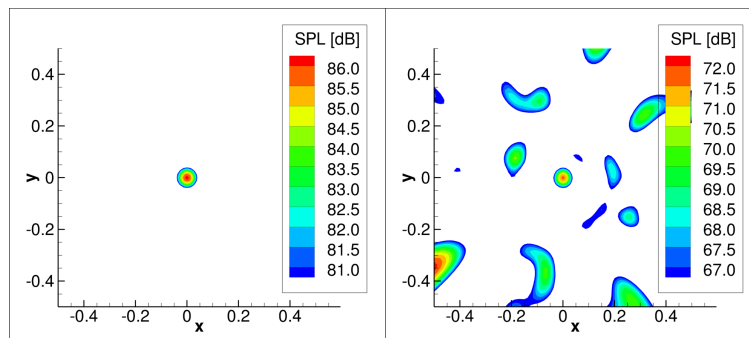


Figure 6: Beamform maps of the simulation case of the rotor noise sources: Absolute reference frame (left), Rotating reference frame (right)

The same noise sources will now be investigated in a rotating reference frame in order to remove the rotation from the rotors, as is customary in turbomachinery investigations. The beamform map for the 15th harmonic of the 15 stationary rotor blades can be seen on the right side of Figure 6. This beamform map is produced by the DS method. After removing the rotation of the noise sources, we are left with 15 stationary coherent noise sources which are evenly distributed around the circumference. The beamform map once again localizes the noise source to a point on the axis, as well as producing many sidelobes in the investigated plane. The 15 coherent noise sources do not appear on the beamform map at their true locations.

While the rotating reference frame removes the already existing rotation from the rotors, it also puts all objects into rotation which would otherwise be stationary. The guide vane is one such object. Figure 7 shows the rotating reference frame beamform maps for the measurement (left side) and simulation (right side) of the guide vane noise source. The measurement data is processed using the ROSI method, and the simulation data is processed using the DS method. Looking at the results for 3000 Hz, it can be seen that a noise source appears on the axis, as is expected according to the Mach radius calculations. Though the noise source is a single rotating noise source that is radiating at 3000 Hz, rotating it at 12000 RPM (200 rev/s) it becomes coherent with itself, producing 15 sections of high and low pressure along the circumference. For each rotation, the pattern is repeated in the same locations. In the measurement results a ring shaped sidelobe can be seen at a radial position halfway between the axis and the rotating guide vane noise source. The simulation results show sidelobe characteristics similar to those seen in Figure 6 for the simulated rotor noise sources also investigated with the DS method.

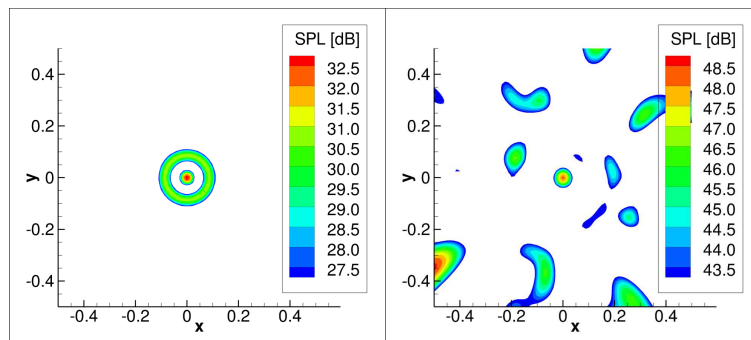


Figure 7: Rotating reference frame beamform maps of the guide vane noise source:
 Measurement case (left) and Simulation case (right)

Rotating reference frame beamform maps for the measurement (left side) and simulation (right side) of the motor noise, which is stationary in both the absolute as well as rotating reference frame, can be seen in Figure 8. The results are very similar to the results seen in the absolute reference frame, though some slight differences can be seen in the levels.

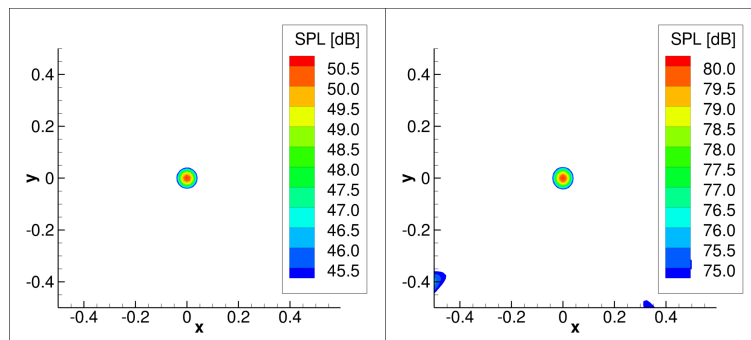


Figure 8: Rotating reference frame beamform maps of the motor noise source:
 Measurement case (left) and Simulation case (right)

The above results present the beamform maps produced by the individual noise sources. In reality these noise sources occur simultaneously. The following sets of figures will compare instances when only the motor, the motor and the guide vane, or the motor, guide vane, and the rotors are simultaneously investigated with beamforming methods.

An investigation of the absolute reference frame simulation results with the ROSI method is looked at in Figure 9. The left side of Figure 9 presents the simulation results for the 15 rotating rotor noise sources. The middle section of Figure 9 presents the simulation results for the 15 rotating rotor noise sources and the stationary guide vane noise source. The right side of Figure 9 presents the simulation results for the 15 rotating rotor noise sources, the stationary guide vane noise source, and the stationary motor noise source. The results show how the levels of the 15 rotating rotor noise

sources and the motor noise source add together when they are investigated simultaneously. If only seeing the results for all three of the noise sources radiating simultaneously (right side of Figure 9) and not taking into account the Mach radius concept, one gets the impression that only the motor and the guide vane are radiating noise, and the motor is the dominant noise source in the investigation. Reemphasizing that all of the monopole noise sources included in the simulation have the same level, this investigation shows that in reality the 15 rotating rotor noise sources made the largest contribution to the noise sources appearing on the beamform maps. The possible noise source and the Mach radius concept cannot be neglected in processing the results.

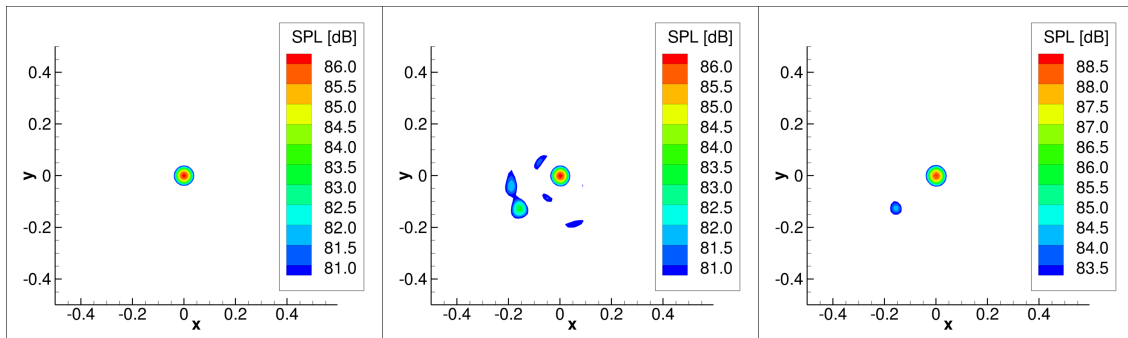


Figure 9: Absolute reference frame beamform maps of the simulation case investigated with the ROSI method: Rotor noise sources (left), rotor noise sources and guide vane noise source (middle), and rotor noise sources, guide vane noise source, and motor noise source (right)

Investigating the same three noise sources in the rotating reference frame is also interesting. Figure 10 presents the simulation results in the rotating reference frame which are investigated by the DS method. The left side of Figure 10 presents the simulation results for the 15 stationary rotor noise sources. The middle section of Figure 10 presents the simulation results for the 15 stationary rotor noise sources and the rotating guide vane noise source. The right side of Figure 10 presents the simulation results for the 15 stationary rotor noise sources, the rotating guide vane noise source, and the stationary motor noise source. Though the sidelobes appearing in these beamform maps dominate the peak values, it can once again be seen that the levels of the three noise sources, all appearing on the axis, add together. The noise sources of the 15 stationary rotor blades and of the guide vane cannot be seen at their true radial positions. If one would not take into account what is known about the Mach radius concept, the results would suggest that the only noise source appearing in the results is the motor. This is especially emphasized since the sidelobes are located at a larger radius than the rotor blade tip, and would therefore be excluded from the investigation. It is once again shown that the Mach radius concept needs to be taken into account when investigating rotating coherent noise sources from the axial direction, regardless of the reference frame in which they are being looked at.

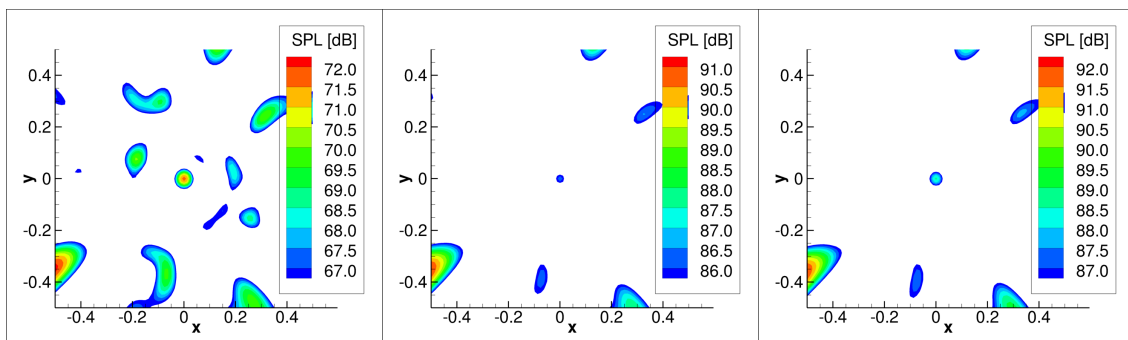


Figure 10: Rotating reference frame beamform maps of the simulation case investigated with the DS method: Rotor noise sources (left), rotor noise sources and guide vane noise source (middle), and rotor noise sources, guide vane noise source, and motor noise source (right)

CONCLUSIONS

The investigation looked at a synthetic axial flow fan test case in order to learn more about the noise sources appearing on the axis. Until now these noise sources were associated with motor noise, but these results show that this is not necessarily the case. The Mach radius concept provides information regarding the origin of these noise sources, and the beamform maps presented in the investigation results confirm that rotating coherent noise sources can produce noise sources that are located on the axis. This information is necessary in order to accurately process beamforming results of rotating coherent as well as incoherent noise sources, and provides the basis of a new beamforming investigation method designed specifically for the investigation of rotating coherent noise sources.

BIBLIOGRAPHY

- [1] P. Sijtsma, S. Oerlemans, H. Holthusen – *Location of rotating sources by phased array measurements*. National Aerospace Lab., Paper NLR-TP-2001-135, **2001**
- [2] W. Pannert, C. Maier – *Rotating beamforming – motion-compensation in the frequency domain and application of high-resolution beamforming algorithms*. Journal of Sound and Vibration, Vol. 333, Issue 7, pp. 1899-1912, **2014**
- [3] J. Kennedy, P. Eret, G. Bennett, P. Castellinni, P. Chiariotti, F. Sopranzetti, C. Picard, A. Finez – *The application of advanced beamforming techniques for the noise characterization of installed counter rotating open rotors*. 19th AIAA/CEAS Aeroacoustics Conference, Paper AIAA 2013-2093, Berlin, Germany, **2013**
- [4] T. Benedek, P. Tóth – *Beamforming measurements of an axial fan in an industrial environment*. Periodica Polytechnica: Mechanical Engineering, Vol. 57, No. 2, pp. 37-46, **2013**
- [5] Cs. Horváth, E. Envia, G. G. Podboy – *Limitations of phased array beamforming in open rotor noise source imaging*. AIAA Journal, Vol. 52, No. 8, pp. 1810-1817, **2014**
- [6] M. J. T. Smith – *Aircraft noise*. Cambridge University Press, **1989**
- [7] T. Mueller, C. Allen, W. K. Blake, R. P. Dougherty, D. Lynch, P. Soderman, J. Underbrink – *Aeroacoustic measurements: chapter 3*. Springer (first edition), **2002**
- [8] A. B. Parry, D. G. Crighton – *Prediction of counter-rotation propeller noise*. AIAA 12th Aeroacoustics Conference, AIAA-89-1141, San Antonio, Texas, **1989**
- [9] E. Envia – *Open rotor aeroacoustic modelling* Conference on Modelling Fluid Flow, Budapest University of Technology and Economics, Budapest, Hungary, pp. 1027-1040, **2012**
- [10] A. Sharma, H. Chen – *Prediction of aerodynamic tonal noise from open rotors* Journal of Sound and Vibration, Vol. 332, No. 16, pp. 3832-3845. doi: 10.1016/j.jsv.2013..02.027, **2013**
- [11] S. W. Rienstra, A. Hirschberg – *An introduction to acoustics*, **2012**
- [12] M. Roger – *Fundamentals of aeroacoustics* von Kármán Institute for Fluid Dynamics Lecture Series 2007-01: Experimental Aeroacoustics, **2006**